

Complete one-loop analysis to stop and sbottom decays into Z and W^\pm bosons

Abdesslam Arhrib^{1,2,3} and Rachid Benbrik²

1. National Center for Theoretical Sciences, PO-Box 2-131 Hsinchu, Taiwan 300
2. LPHEA, Faculté des Sciences-Semlalia, B.P. 2390 Marrakech, Morocco.
3. Faculté des Sciences et Techniques de Tanger, B.P 416 Tanger, Morocco.

Abstract

We study radiative corrections to third generation scalar fermions into gauge bosons Z and W^\pm . We include both SUSY-QCD, QED and full electroweak corrections. It is found that the electroweak corrections can be of the same order as the SUSY-QCD corrections and interfere destructively in some region of parameter space. The full one loop correction can reach 10% in some SUGRA scenario, while in general MSSM, the one loop correction can reach 20% for large $\tan\beta$ and large trilinear soft breaking terms A_b .

1. Supersymmetric theories predict the existence of scalar partners to all known quarks and leptons. In Grand unified SUSY models, the third generation of scalar fermions, $\tilde{t}, \tilde{b}, \tilde{\tau}$, gets a special status; due to the influence of Yukawa-coupling evolution, the light scalar fermions of the third generation are expected to be lighter than the scalar fermions of the first and second generations. For the same reason, the splitting between the physical masses of the third generation may be large enough to allow the opening of the decay channels like : $\tilde{f}_2 \rightarrow \tilde{f}_1 V$ and/or $\tilde{f}_2 \rightarrow \tilde{f}_1 \Phi$, where V is a gauge boson and Φ is a scalar boson.

Until now there is no direct evidence for SUSY particles, and under some assumptions on their decay rates, one can only set lower limits on their masses [1]. It is expected that the next generation of e^+e^- machines and/or hadron colliders (LHC and Tevatron) could establish the first evidence for the existence of SUSY particles if they are not too heavy.

If SUSY particles would be detected at hadron colliders, their properties can be studied with high accuracy at a high-energy linear e^+e^- collider [2]. It is thus mandatory to incorporate effects beyond leading order into the theoretical predictions, both for production and decay rate, in order to match the experimental accuracy.

In this spirit, radiative corrections to the decays of SUSY particles have been carried out. In particular, the QCD corrections to scalar quark decay into quarks plus charginos or neutralinos have been studied in [3], while the full one loop analysis has been addressed in [4] and found to have important impact on the partial decay widths of scalar fermions. The QCD corrections to the decays of heavy scalar quarks into light scalar quarks and Higgs bosons are found to be important [5].

Obviously, most of the studies concentrated on the production and decay of light states \tilde{t}_1, \tilde{b}_1 and $\tilde{\tau}_1$, while heavier states received less attention [4, 5, 6, 7]. These heavy states can be produced both at LHC and/or at the future e^+e^- linear colliders. The decay of the heavier states third generation scalar fermions is more complicated than the light one. One can basically have four set of two-body decays: i) Strong decay for stop and sbottom $\tilde{t}_2 \rightarrow t\tilde{g}$, $\tilde{b}_2 \rightarrow b\tilde{g}$: if these decay are kinematically open they are the dominant one. ii) decay to chargino and neutralino : $\tilde{f}_2 \rightarrow f\tilde{\chi}_i^0$, $\tilde{f}_2 \rightarrow f'\tilde{\chi}_i^+$.

If the splitting between light and heavy third generation scalar fermions is large enough

we may have the following decays: iii) $\tilde{f}_2 \rightarrow \tilde{f}_1 \Phi^0$, $\Phi^0 = h^0, H^0, A^0$, and $\tilde{f}_2 \rightarrow \tilde{f}'_1 H^\pm$. iv) $\tilde{f}_2 \rightarrow \tilde{f}_1 Z^0$ and $\tilde{f}_2 \rightarrow \tilde{f}'_1 W^\pm$.

In the MSSM, the decay modes $\tilde{f}_2 \rightarrow \tilde{f}_1 Z^0$ and $\tilde{f}_i \rightarrow \tilde{f}'_j W$, if open and under some assumptions, may be the dominant one. Note also that in several benchmarks scenarios for SUSY searches, the bosonic decay of \tilde{t}_i and \tilde{b}_i may be the dominant [8]. For example, in SPS5 scenario the dominant bosonic decay have the following branching ratios [8]: $Br(\tilde{b}_1 \rightarrow W^- \tilde{t}_1) = 81\%$, $Br(\tilde{b}_2 \rightarrow W^- \tilde{t}_1) = 64\%$ and $Br(\tilde{t}_2 \rightarrow Z^0 \tilde{t}_1) = 61\%$. While in SPS1 scenario, we have: $Br(\tilde{b}_2 \rightarrow W^- \tilde{t}_1) = 34\%$ and $Br(\tilde{t}_2 \rightarrow Z^0 \tilde{t}_1) = 23\%$.

Here, we provide the complete one loop radiative corrections to $\tilde{f}_2 \rightarrow \tilde{f}_1 Z^0$ and $\tilde{f}_i \rightarrow \tilde{f}'_j W$ including real photon emission [9], and discuss their effects in combination with the SUSY-QCD corrections [10]. We show that SUSY-QCD corrections can interfere destructively with electroweak one.

2. The tree-level decay width for $\tilde{q}_i^\alpha \rightarrow \tilde{q}_j^\beta V$ can thus be written as:

$$\Gamma^0(\tilde{q}_i^\alpha \rightarrow \tilde{q}_j^\beta V) = \frac{(g_{V\tilde{f}_i\tilde{f}_j})^2 \kappa^3(m_i^2, m_j^2, m_V^2)}{16\pi m_V^2 m_i^3}, \quad (1)$$

with $\kappa(x, y, z) = (x^2 + y^2 + z^2 - 2xy - 2xz - 2yz)^{1/2}$, $g_{Z\tilde{f}_i\tilde{f}_j} = \frac{e}{s_W c_W} \{(I_3^f - Q_f s_W^2) \sin \theta_f \cos \theta_f + Q_f s_W^2 \cos \theta_f \sin \theta_f\}$, $g_{Z\tilde{f}_i\tilde{f}_j} = g_{Z\tilde{f}_i\tilde{f}_i}$ and $g_{W\tilde{f}_i\tilde{f}'_j} = \frac{e}{\sqrt{2}s_W} \cos \theta_f \sin \theta_{f'}$, I_3^f is the isospin.

At one loop level, the decay $\tilde{q}_i^\alpha \rightarrow \tilde{q}_j^\beta V$ receive contributions from vertex diagrams, gauge boson V and scalar fermions \tilde{q}_i^α self energies as well as their mixings (see [9] for details). Note that the transitions between gauge bosons and scalar bosons like W^\pm - H^\pm , W^\pm - G^\pm , Z^0 - A^0 , Z^0 - G^0 are present. Owing to Lorentz invariance, those mixing are proportional to p_V^μ momentum; then since the vector gauge bosons W and Z are on-shell transverse, those transitions vanish. In what follows we will ignore vector-scalar boson mixing.

We have evaluated the one-loop amplitudes in the 't Hooft-Feynman gauge using FeynArts and FormCalc [13, 14]. The one-loop amplitudes are ultraviolet (UV) and infrared (IR) divergent. The UV singularities are treated by dimensional reduction and are compensated in the on-shell renormalization scheme. We have checked explicitly that the results are identical in using dimensional reduction and dimensional regularization. The IR singularities are regularized with a small fictitious photon mass δ and are eliminated by adding to the one loop contribution both real-photon and real-gluon emission [9], $\tilde{f}_i \rightarrow \tilde{f}_j^* V \gamma$ and $\tilde{f}_i \rightarrow \tilde{f}_j^* V g$.

Recently, there have been several developments in the renormalization of MSSM. Several schemes are available [16]. Here, we follow the strategy of [4, 7] by introducing counter-terms for the physical parameters, i.e. for masses and mixing angles, and perform field renormalization in a way that residues of renormalized propagators can be kept at unity. For SM parameters and fields, we will adopt throughout, the on-shell renormalization scheme of Refs. [15]. In the on-shell scheme we use the mixing angle s_W (resp c_W) is defined by $s_W^2 = 1 - M_W^2/M_Z^2$ (resp $c_W^2 = M_W^2/M_Z^2$). Its counter-term is completely fixed by the mass counter-terms of W and Z gauge bosons.

The extra parameters and fields we still have to renormalize in our case are the scalar fermion wave functions \tilde{f}_i and the mixing angle θ_f which enter in the tree level amplitude eq. (1).

In the general case, where sfermions mixing is allowed, the wave functions of the two sfermions mass eigenstates are not decoupled. Taking into account the mixing, the renormalization of the sfermions wave functions and the mixing angle θ_f can be performed by making the following substitutions in the Lagrangian

$$\tilde{f}_1 \rightarrow Z_{11}^{1/2} \tilde{f}_1 + Z_{12}^{1/2} \tilde{f}_2 \quad , \quad \tilde{f}_2 \rightarrow Z_{22}^{1/2} \tilde{f}_2 + Z_{21}^{1/2} \tilde{f}_1 \quad , \quad \theta_f \rightarrow \theta_f + \delta\theta_f \quad (2)$$

To fix all the renormalization constants, we use the following renormalization conditions:

i) The on-shell conditions for m_W , m_Z , m_e and the electric charge e are defined as in the Standard Model [15].

ii) On-shell condition for the scalar fermion \tilde{f}_i : we choose to identify the physical scalar fermion mass with the corresponding parameter in the renormalized Lagrangian, and require the residue of the propagators to have its tree-level value, i.e.,

$$\delta Z_{ii} = -\Re\left\{\frac{\partial}{\partial p^2}(\Sigma_{\tilde{f}_i\tilde{f}_i}(p^2))\right\}\Big|_{p^2=m_{\tilde{f}_i}^2} \quad , \quad \delta Z_{ij} = \frac{\Re\{\Sigma_{\tilde{f}_i\tilde{f}_j}(m_{\tilde{f}_j}^2)\}}{m_{\tilde{f}_j}^2 - m_{\tilde{f}_i}^2} \quad , \quad \delta m_{\tilde{f}_i}^2 = \Re(\Sigma_{\tilde{f}_i\tilde{f}_j}(m_{\tilde{f}_i}^2)) \quad (3)$$

where $\Sigma_{\tilde{f}_i\tilde{f}_j}(p^2)$, $i, j = 1, 2$ is the scalar fermion bare self-energy.

iii) For the renormalization condition which defines the mixing angle θ_f , we select this condition in such a way to kill the transitions $\tilde{f}_i \leftrightarrow \tilde{f}_j$ at the one-loop level. The renormalization of the scalar fermion mixing angle is then given by [4]:

$$\delta\theta_f = \frac{1}{2} \frac{\Sigma_{\tilde{f}_i\tilde{f}_j}(m_{\tilde{f}_j}^2) + \Sigma_{\tilde{f}_i\tilde{f}_j}(m_{\tilde{f}_i}^2)}{m_{\tilde{f}_j}^2 - m_{\tilde{f}_i}^2} \quad (4)$$

3. Now we are ready to present our numerical results both for the tree-level and one-loop decay widths and branching ratios for $\tilde{f}_i \rightarrow \tilde{f}_j Z$ and $\tilde{f}_i \rightarrow \tilde{f}'_j W^\pm$. Let us first fix our inputs and SUSY parameters choice.

As experimental data points, the following input quantities enter: $\alpha^{-1} = 137.03598$, $m_Z = 91.1875$ GeV, $m_W = 80.45$ GeV. For quarks masses, we use effective quark masses that reproduce the hadronic vacuum polarization contribution $\Delta\alpha(m_Z^2)$ with a sufficiently high accuracy have been chosen [17].

For the SUSY parameters, we will use MSSM inputs which look like some of the Snow-mass Points and Slopes (SPS) and benchmarks scenarios for SUSY searches [8]. For our study we will use SPS1 and SPS5 scenario. As we explained in the introduction, for those 2 scenarios the bosonic decays of scalar fermions $\tilde{f}_i \rightarrow \tilde{f}_j V$, when open, are dominant.

In SPS1, we have the following spectrum (are listed only the parameters needed): $\tan\beta = 10$, $m_{A^0} = 394$ GeV, $A_t = -431.34$ GeV, $A_b = 582.67$ GeV, $M = 193$ GeV, $M' = 99$ GeV, $\mu = 352$ GeV. The mass of the first and second generation scalar fermion is of the order 177 GeV (average). While the masses of the third generation scalar fermions are : $m_{\tilde{t}_1} = 396.43$ GeV, $m_{\tilde{t}_2} = 574.71$ GeV, $m_{\tilde{b}_1} = 491.91$ GeV, $m_{\tilde{b}_2} = 524.59$ GeV. The mixing angle are given by $\cos\theta_t = 0.57$, $\cos\theta_b = 0.88$.

In SPS5 (light stop scenario), we have the following spectrum : $m_{A^0} = 694$ GeV, $\tan\beta = 5$, $A_t = -785.57$ GeV, $A_b = -139.11$ GeV, $M = 235$ GeV, $M' = 121$ GeV, $\mu = 640$ GeV. The mass of the first and second generation scalar fermion is of the order 231 GeV (average). The masses of the third generation are $m_{\tilde{t}_1} = 253.66$ GeV, $m_{\tilde{t}_2} = 644.65$ GeV, $m_{\tilde{b}_1} = 535.86$ GeV, $m_{\tilde{b}_2} = 622.99$ GeV. The mixing angle are given by $\cos\theta_t = 0.54$, $\cos\theta_b = 0.98$.

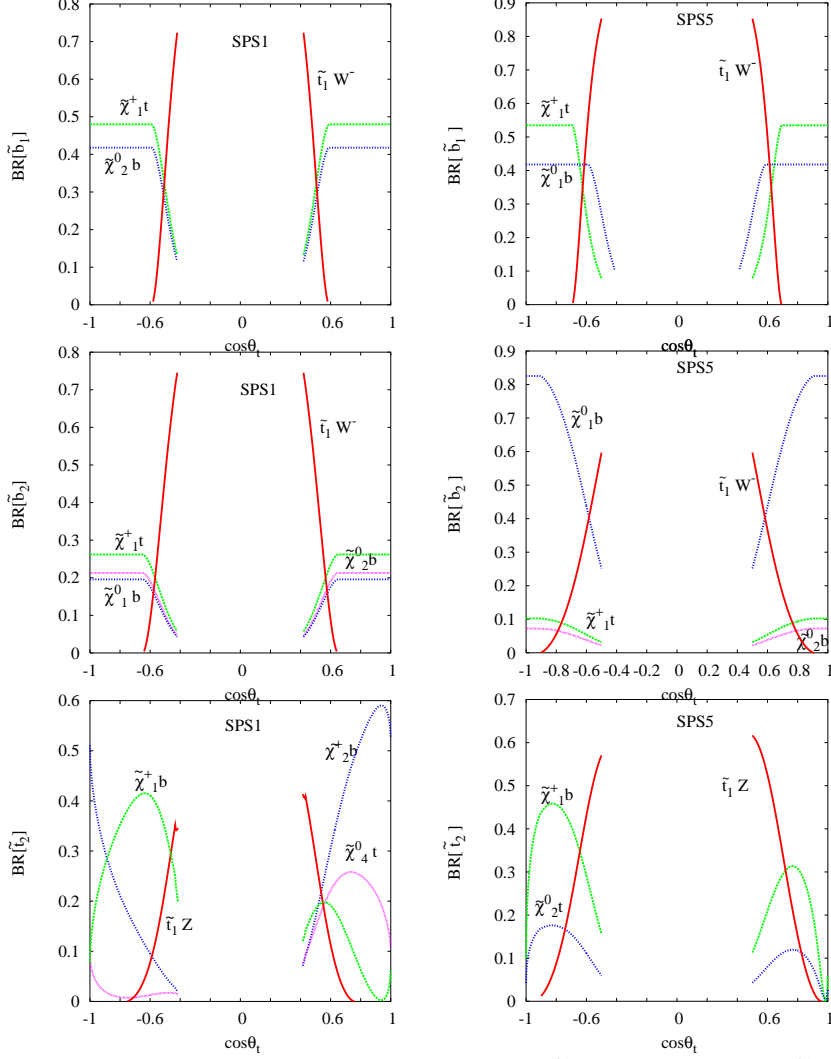


Figure 1: Branching ratios of bosonic decays of \tilde{b}_1 (upper plots), \tilde{b}_2 (middle plots) and \tilde{t}_2 (lower plots) in SPS1 (left) and SPS5 (right) as function of $\cos\theta_t$.

In fact, our strategy is the following : the SPS1 and SPS5 outputs are fixed as above, but we will allow a variation of the mixing angles $\cos\theta_t$, $\cos\theta_b$ from their SPS values. According to our parametrization defined in section 2, we choose as independent parameters $m_{\tilde{t}_2}$, $m_{\tilde{b}_1}$, $m_{\tilde{b}_2}$, θ_t , θ_b together with μ and $\tan\beta$. $m_{\tilde{t}_1}$ and A_f are fixed by

$$m_{\tilde{t}_1}^2 = \frac{1}{\cos^2\theta_t} (m_W^2 \cos 2\beta - m_{\tilde{t}_2}^2 \sin^2\theta_t + m_{\tilde{b}_2}^2 \sin^2\theta_b + m_{\tilde{b}_1}^2 \cos^2\theta_b + m_t^2 - m_b^2) \quad (5)$$

$$A_f = \mu (\tan\beta)^{-2I_f} + \frac{m_{f_1}^2 - m_{f_2}^2}{m_f} \sin\theta_f \cos\theta_f \quad (6)$$

The variation of $\cos\theta_t$ and $\cos\theta_b$ imply the variation of $m_{\tilde{t}_2}$ as well as A_t and A_b . Since we allow variation of the $\cos\theta_t$ and $m_{\tilde{t}_2}$ mass, our inputs can be viewed as a general MSSM inputs and not as SPS one.

As outlined in section 2, $A_{t,b}$ are fixed by tree level relation eq. (6). Of course, $A_{t,b}$ receive radiative corrections at high order. However, A_t and A_b enter game only at one-loop level in our processes, radiative corrections to A_t and A_b is considered as two-loop effects.

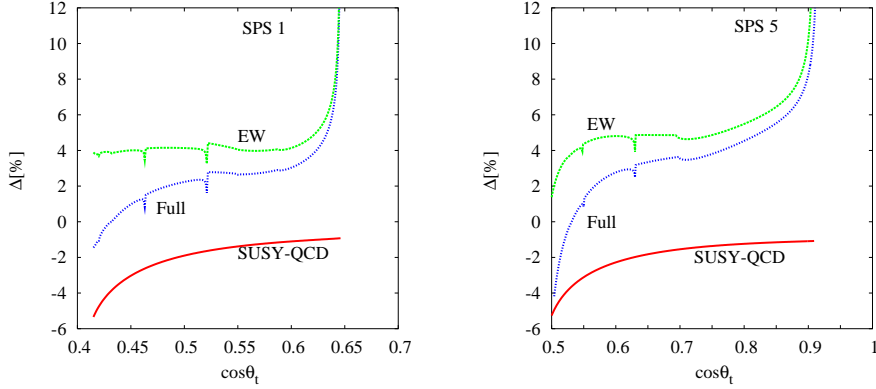


Figure 2: Relative correction (electroweak EW, SUSY-QCD and full) to $\tilde{b}_2 \rightarrow \tilde{t}_1 W$ as function of $\cos \theta_t$ in SPS1 (left) and SPS5 (right)

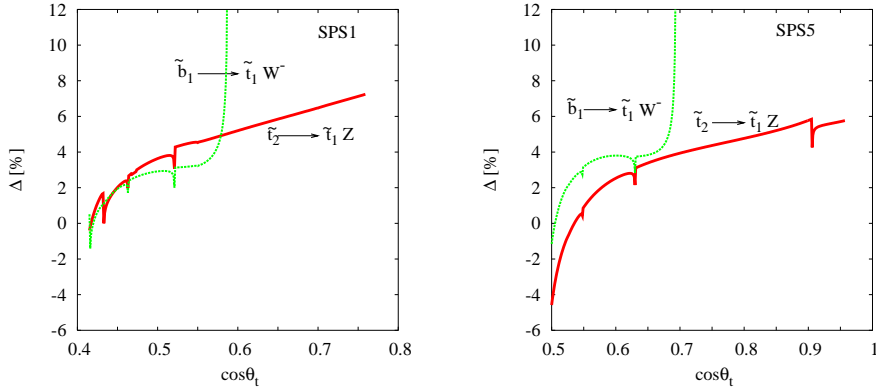


Figure 3: Relative correction to $\tilde{b}_1 \rightarrow \tilde{t}_1 W$ and $\tilde{t}_2 \rightarrow \tilde{t}_1 Z$ as function of $\cos \theta_t$ in SPS1 (left) and SPS5 (right)

In Fig. (1) we show branching ratios of \tilde{b}_1 , \tilde{b}_2 and \tilde{t}_2 . We evaluate the bosonic decays : $\tilde{b}_1 \rightarrow W^- \tilde{t}_1$, $\tilde{b}_2 \rightarrow W^- \tilde{t}_1$ and $\tilde{t}_2 \rightarrow Z^0 \tilde{t}_1$ as well as the fermionic decays $\tilde{f}_i \rightarrow \chi_i^0 f (\chi_i^+ f')$ as function of $\cos \theta_t$ for SPS1 (left) and SPS5 (right) scenario. From those plots, it is clear that the bosonic decay, once open, are the dominant one for $|\cos \theta_t| \approx 0.4 \rightarrow 0.45$. For $|\cos \theta_t| \approx 0.4$ the light stop $m_{\tilde{t}_1}$ is about 100 GeV, when $|\cos \theta_t|$ increases, the $m_{\tilde{t}_1}$ increases also and for large $|\cos \theta_t|$ the bosonic decays are already close and the branching ratio vanishes.

We note that in the case of SPS1 the bosonic decays are open only for $0.4 \lesssim |\cos \theta_t| \lesssim 0.6$ Fig .(1) (left). In the region $|\cos \theta_t| \lesssim 0.4$, the light stop is below the experimental upper limit $m_{\tilde{t}_1} \approx 90$ GeV, and no data are shown. While in the case of SPS5 Fig .(1) (right), for $|\cos \theta_t| \lesssim 0.5$, we find that $m_{\tilde{t}_1}$ is below the experimental upper limit and also $\delta \rho \gtrsim 0.001$ due to large splitting between stops and sbottoms.

The magnitude of SUSY radiative corrections can be described by the relative correction which we define as:

$$\Delta = \frac{\Gamma^{1\text{-loop}}(\tilde{f}_i \rightarrow \tilde{f}_j V) - \Gamma^{\text{tree}}(\tilde{f}_i \rightarrow \tilde{f}_j V)}{\Gamma^{\text{tree}}(\tilde{f}_i \rightarrow \tilde{f}_j V)} \quad (7)$$

In Fig. (2) we illustrate the relative correction Δ as function of $\cos \theta_t$ for the decay $\tilde{b}_2 \rightarrow W \tilde{t}_1$ in SPS1 (left) and SPS5 (right). As it can be seen from the left plot, the SUSY-

QCD corrections [18] lies in the range $-1\% \rightarrow -6\%$ while the EW corrections lie in the range $4\% \rightarrow 10\%$ for $\cos\theta_t \approx 0.4 \rightarrow 0.65$. The SUSY-QCD and EW corrections are of opposite sign, there is a destructive interference and so the full one-loop corrections lie between them. For $\cos\theta_t \rightarrow 0.65$, the total correction increases to about 10%. This is due to the fact that for $\cos\theta_t \rightarrow 0.65$ the mass of light stop is $m_{\tilde{t}_1} \approx 444$ GeV, the decay $\tilde{b}_2 \rightarrow W\tilde{t}_1$ is closed and so the tree level width decreases to zero. The observed peaks around $\cos\theta_t \approx 0.46$ (resp $\cos\theta_t \approx 0.53$) correspond to the opening of the transition $\tilde{t}_1 \rightarrow \chi_1^0 t$ (resp $\tilde{t}_1 \rightarrow \chi_2^0 t$). The right plot of Fig. (2) in SPS5 scenario, exhibits almost the same behavior as the left plot. The electroweak corrections interfere destructively with the SUSY-QCD ones, the full corrections are between $-4\% \rightarrow 10\%$ for $\cos\theta_t \in [0.5, 0.9]$.

In Fig. (3) we show the relative correction Δ as function of $\cos\theta_t$ for the decay $\tilde{b}_1 \rightarrow W\tilde{t}_1$ and $\tilde{t}_2 \rightarrow Z\tilde{t}_1$ in SPS1 (left) and SPS5 (right) scenario.

In the case of $\tilde{t}_2 \rightarrow Z\tilde{t}_1$, the total correction lies in $-1 \rightarrow 7\%$ (resp $-5 \rightarrow 6\%$) in SPS1 (resp SPS5) scenario. From Fig. (3), one can see that the relative corrections for $\tilde{b}_1 \rightarrow W\tilde{t}_1$ are enhanced for $\cos\theta_t \approx 0.6$ (resp $\cos\theta_t \approx 0.75$) in SPS1 (resp SPS5). This behavior has the same explanation as for $\tilde{b}_2 \rightarrow W\tilde{t}_1$ in figure. (2). At $\cos\theta_t \approx 0.6$ (resp $\cos\theta_t \approx 0.75$) in SPS1 (resp SPS5), the decay channel $\tilde{b}_1 \rightarrow W\tilde{t}_1$ (resp $\tilde{t}_2 \rightarrow Z\tilde{t}_1$) is closed and so the tree level width decreases to zero. The observed peaks around $\cos\theta_t \approx 0.46$ (resp $\cos\theta_t \approx 0.53$) correspond to the opening of the transition $\tilde{t}_1 \rightarrow \chi_1^0 t$ (resp $\tilde{t}_1 \rightarrow \chi_2^0 t$).

In all cases, we have isolated the QED corrections (virtual photons and real photons), we have checked that this contribution is very small, less than about 1%.

Fig.(4) illustrates the relative corrections to $\tilde{t}_2 \rightarrow \tilde{b}_1 W$, $\tilde{t}_2 \rightarrow \tilde{t}_1 Z$ (left) and $\tilde{b}_2 \rightarrow \tilde{b}_1 Z$, $\tilde{b}_2 \rightarrow \tilde{t}_1 W$ (right) as function of $A_b = A_t$ in general MSSM for large $\tan\beta = 60$, $\mu = 500$ GeV, $M_2 = 130$ GeV and $M_A = 200$ GeV. It is clear from this plot that the relative corrections are bigger than in the cases of SPS scenarios. This enhancement shows up for large $|A_b|$ and also near threshold regions. In this scenario, the SUSY-QCD corrections are about 2%, the electroweak corrections are about 5% while the QED corrections are very small. The dominant contribution comes from the Yukawa corrections and is enhanced by large $\tan\beta = 60$ and large $|A_b|$.

In the left plot of Fig.(4), the region $|A_b| = |A_t| < 300$ GeV has no data. This is due to the fact that splitting between \tilde{t}_2 and \tilde{t}_1 (\tilde{t}_2 and \tilde{b}_1) is not large enough to allow the decays $\tilde{t}_2 \rightarrow \tilde{t}_1 Z$ and $\tilde{t}_2 \rightarrow \tilde{b}_1 W$.

In the right plot of Fig.(4), when $|A_b| = |A_t| \approx 0$ GeV, the splitting between \tilde{b}_2 and \tilde{t}_1 is close to m_W mass and so the tree level width for $\tilde{b}_2 \rightarrow \tilde{t}_1 W^+$ almost vanish, consequently the correction is getting bigger. This behavior has been also observed in previous plots for $\tilde{b}_2 \rightarrow \tilde{t}_1 W^+$.

Finally, in Fig. (5) we illustrate the decay width of $\tilde{t}_2 \rightarrow \tilde{t}_1 Z$ as function of $m_{\tilde{t}_1}$ in SPS1 (left) and SPS5 (right). In SPS1 (resp SPS5) the decay width of $\tilde{t}_2 \rightarrow \tilde{t}_1 Z$ is about 8 GeV (resp 13 GeV) for light stop mass of the order 100 GeV. Obviously, these decays width decrease as the light stop mass increase.

It is clear that the SUSY-QCD corrections reduces the width while the electroweak corrections cancel part of those QCD corrections. Both in SPS1 and SPS5, the full one loop width of $\tilde{t}_2 \rightarrow \tilde{t}_1 Z$ is in some case slightly bigger than the tree level width.

4. To conclude, a full one-loop calculations of third-generation scalar-fermion decays into

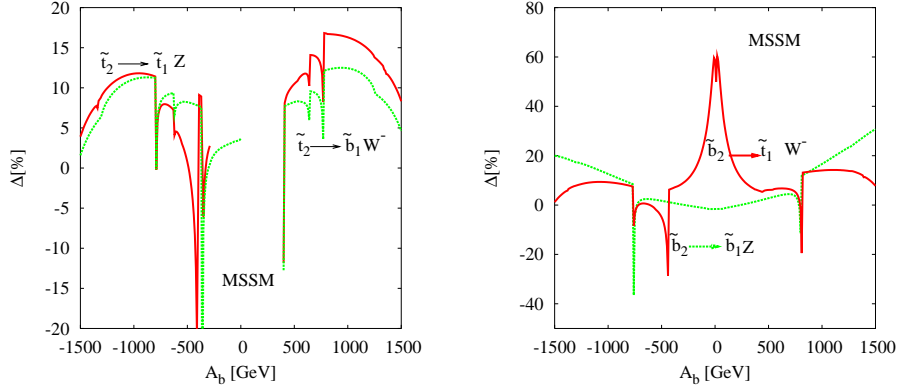


Figure 4: Relative correction to $\tilde{t}_2 \rightarrow \tilde{b}_1 W, \tilde{t}_2 \rightarrow \tilde{t}_1 Z$ (left) and $\tilde{b}_2 \rightarrow \tilde{b}_1 Z, \tilde{b}_2 \rightarrow \tilde{t}_1 W$ (right) as function of $A_t = A_b$ in MSSM for $\mu, M_2, M_A = 500, 130, 200$ GeV and $\tan \beta = 60$

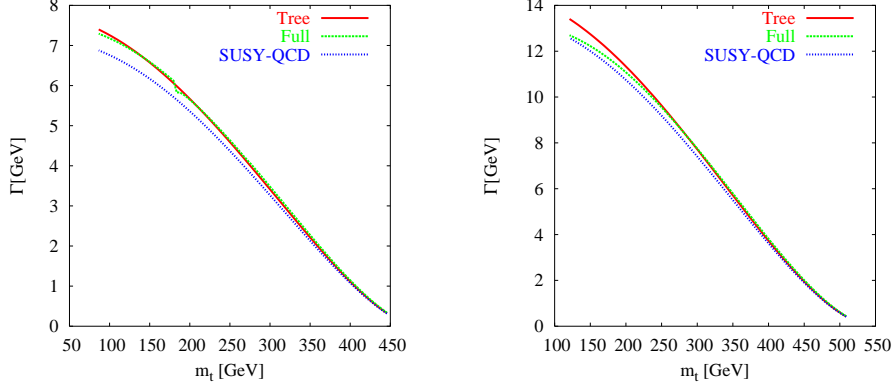


Figure 5: Tree and one loop decay width of $\tilde{t}_2 \rightarrow \tilde{t}_1 Z$ as function of $m_{\tilde{t}_1}$

gauge bosons W and Z are presented in the on-shell scheme. We include both electroweak, QED and SUSY-QCD contributions to the decay width. It is found that the electroweak and SUSY-QCD corrections interfere destructively.

The size of the one-loop effects are typically of the order $-5\% \rightarrow 10\%$ in SPS scenarios which are based on SUGRA assumptions. While in the general MSSM, the size of the corrections are bigger and can reach about 20% for large $\tan \beta$ and large soft SUSY breaking A_b . Their inclusion in phenomenological studies and analyses are then well motivated.

Acknowledgment:

We are very grateful to Prof. Mohamed Chabab and the Organizing committee for the invitation to ICHEMP05 and for the kind hospitality at Cadi Ayyad University. A.A is supported by the Physics Division of National Center for Theoretical Sciences under a grant from the National Science Council of Taiwan. This work is supported by PROTARS-III D16/04.

References

- [1] T. Affolder *et al*, Phys. Rev. D **63**, 091101 (2001); G. Abbiendi *et al*, Phys. Lett. B **545**, 272 (2002) [Erratum-ibid. B **548**, 258 (2002)];
- [2] J. A. Aguilar-Saavedra *et al*, arXiv:hep-ph/0106315; K. Abe *et al*, arXiv:hep-ph/0109166; T. Abe *et al*, arXiv:hep-ex/0106056.
- [3] A. Djouadi, W. Hollik and C. Junger, Phys. Rev. D **55**, 6975 (1997); S. Kraml, H. Eberl, A. Bartl, W. Majerotto and W. Porod, Phys. Lett. B **386**, 175 (1996).
- [4] J. Guasch, W. Hollik and J. Sola, order," JHEP **0210**, 040 (2002); J. Guasch, J. Sola and W. Hollik, Phys. Lett. B **437**, 88 (1998);
- [5] A. Arhrib, A. Djouadi, W. Hollik and C. Junger, Phys. Rev. D **57**, 5860 (1998).
- [6] A. Bartl et al, Z. Phys. C **76**, 549 (1997).
- [7] A. Arhrib and W. Hollik, JHEP **0404**, 073 (2004).
- [8] B. C. Allanach *et al.*, Eur. Phys. J. C **25**, 113 (2002); N. Ghodbane and H. U. Martyn, arXiv:hep-ph/0201233.
- [9] A. Arhrib and R. Benbrik, Phys. Rev. D **71**, 095001 (2005).
- [10] A. Bartl et al bosons," Phys. Lett. B **419**, 243 (1998).
- [11] A. Djouadi, J. L. Kneur and G. Moultaka, arXiv:hep-ph/0211331.
- [12] M. Muhlleitner, A. Djouadi and Y. Mambrini, particles in the arXiv:hep-ph/0311167.
- [13] J. Kublbeck, M. Bohm, A. Denner, Comput. Phys. Commun. **60**, 165 (1990); T. Hahn, Comput. Phys. Commun. **140**, 418 (2001); T. Hahn, C. Schappacher, Comput. Phys. Commun. **143**, 54 (2002); T. Hahn et al, Comput. Phys. Commun. **118**, 153 (1999);
- [14] G. J. van Oldenborgh, Comput. Phys. Commun. **66**, 1 (1991); T. Hahn, Acta Phys. Polon. B **30**, 3469 (1999)
- [15] A. Denner, Lep-200," Fortsch. Phys. **41**, 307 (1993).
- [16] W. Hollik et al, Nucl. Phys. B **639**, 3 (2002); W. Majerotto, arXiv:hep-ph/0209137; T. Fritzsche and W. Hollik, Eur. Phys. J. C **24**, 619 (2002);
- [17] S. Eidelman and F. Jegerlehner, *Z. Phys.* **C67** (1995) 585–602.
- [18] A. Arhrib, M. Capdequi-Peyranere and A. Djouadi, Phys. Rev. D **52**, 1404 (1995). H. Eberl, A. Bartl and W. Majerotto, Nucl. Phys. B **472**, 481 (1996).